HYDROGEN DEPTH PROFILE IN GENESIS DOS COLLECTORS. H. Yurimoto[1, 2], N. Sakamoto[1], K. Bajo[1], A. J. G. Jurewicz[3] and D. S. Burnet[4], [1]Depertment of Natural History Sciences, Hokkaido University, IIL, Sapporo 001-0021, Japan (yuri@ep.sci.hokudai.ac.jp), [2]ISAS/JAXA, Sagamihara 252-5210, Japan, [3]CMS/SESE, Arizona State University, Tempe, AZ 85287-1404, USA, [4]Division of Geological and Planetary Sciences, California Institute of Technology, Pasadena, CA 91125, USA.

Introduction: The highest energies of solar wind (SW) H and He give insight into the solar phenomenon known as a coronal mass ejection (CME). These high energies can be measured in *Genesis* samples, as the implantation profiles of SW particles in a solid material directly irradiated by the SW echo that energy distribution. We previously measured a SW He implantation profile from a bulk solar wind collector from the NASA *Genesis* SW sample return mission [1, 2] and discussed energy distribution of SW components for the low-speed, high-speed and coronal mass ejection (CME) He. Here we present results for SW H.

Hydrogen is the most abundant element in the SW and analyses producing depth profile analysis of SW H have been used successfully to determine the H fluence [3, 4]; however, fluence analyses do not require a wide dynamic range, so their analysis of the energy distribution of SW H is limited. Here we report depth profiles of SW H from bulk solar wind and CME collectors of *Genesis* that have a wide dynamic range.

Experimental: Collector chips of diamond-like carbon film on silicon wafer (DOS) from the *Genesis* B/C and E arrays were measured. The chips allocated were: #61330 from the B/C bulk solar wind array and #61921 from the coronal mass ejection (CME) E array. The chips were placed in ultra-high vacuum ($1x10^{-7}$ Pa) for about one month before measurement in order to reduce adsorbed water before placing them into the sample chamber ($6x10^{-8}$ Pa) for measurement. A cold trap of liquid nitrogen was used to reduce water vapor pressure in the sample chamber.

The *Genesis* collector chips were measured by secondary ion mass spectrometry in depth-profiling mode using Cameca ims 1270 at Hokkaido University. We applied focused Cs^+ ion primary beam (~5 μm in diameter) of current of 10 nA with total kinetic energy of 15 keV. The primary beam was rastered 25 x 25 μm^2 to form a flat bottom crater on the sample surface. Secondary ions of $^{13}C^-$ and $^{12}CH^-$ sputtered from the central area of 5 × 10 μm^2 was selected by the field aperture in order to reduce possible crater-edge effects, and accelerated to 5 keV, and was measured using an electron multiplier (EM) by peak jumping mode of sector magnet. The small contrast aperture of 100 μm and narrow energy slit band-pass of 25 eV was applied to improve the spatial resolution of the secondary ion image of 0.5 μm, as a result, to reduce possible contamination of H intensities from surface absorbed water due to optical flare and aberration. The mass resolution power (MRP) of M/ΔM was set at ~5600 to ensure that the contribution of $^{13}C^-$ to $^{12}CH^-$ is negligible. The EM was operated in pulse counting mode with a dead time of 27 ns. A typical count rate of $^{13}C^-$ was 10^5 cps, which is larger than for $^{12}CH^-$, so that the counting loss of both ions due to dead time was negligible. A typical counting sequence with $^{13}C^-$ for 0.5 s and $^{12}CH^-$ for 2 s with a waiting time of 1 s for every mass to stabilize the sector magnetic field. Typical measurement time for an in depth profile was 5 minutes. Differences of primary beam currents before and after in depth-analysis were less than 5 % (less than 2 % for most cases).

Crater depths were measured after depth profiling analyses by a laser microscope (Keyence VK-X200) at Hokkaido University. The sputter time was converted to depth assuming constant sputter rate for each crater.

Results and discussion: A typical depth profile of SW H in DOS collector is shown in Fig. 1. The stable signal of ^{13}C, which is the matrix element of diamond-like carbon, indicates that secondary emission is stable through the in-depth analysis. The SW H is measured using the signal of the molecular ion ^{12}CH. The ^{12}CH signal decreased with increasing depth to several tens cps. The small peaks of ^{12}CH around 200 and 400 nm in depth (showed by arrows) are not artifacts. This peak appears cyclically every 200 nm reflecting fabrication process of the diamond-like carbon layer. Small variations in the ^{12}CH signal deeper than 250 nm also show variations in hydrogen intrinsic to the diamond-like carbon (as fabricated) because the same pattern appears in duplicate measurements.

Using the known fluence for SW H in the B/C array [4], secondary ion ratios of $^{12}CH/^{13}C$ were translated to H concentration. Duplicate measurements (~10 per array) were combined into one depth profile for that array (Fig. 2). Using these combined profiles gives the following results. The intrinsic hydrogen content of diamond-like carbon is 1.5×10^{18} cm^{-3} (30 ppma). The depth profiles in both arrays have different peak H concentrations but similar peak depths: 6.0×10^{21} cm^{-3} at 12 nm in depth for B/C array, 1.5×10^{21} cm^{-3} at 14 nm for E array. The peak depths indicate that both arrays collected SW H at an dominant energy of ~1 keV; that is because the algorithm for *Genesis* array de-

ployment put any suspect low- and high speed SW into the E array in addition to SW from CMEs [5]. The H concentration drops to ~10^{19} cm^{-3} at 100 nm; after that the rate of decrease slows to show high-energy SW H tails. The tail profiles are essentially the same between both profiles. Similar tailing has been observed from the He depth profile of *Genesis* DOS target [2].

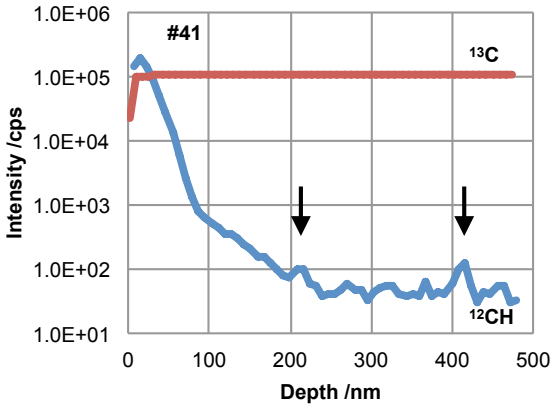

Figure 1. Depth profile of solar wind hydrogen in Genesis B/C DOS collector.

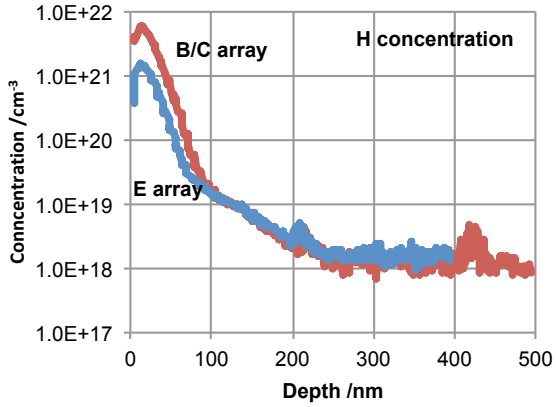

Figure 2. Concentration profile of solar wind hydrogen in Genesis B/C and E DOS collectors.

The ratio of E/(B/C) fluences we measure is 0.251 vs. (0.243) from [4], a 3% difference which may be real. If so, the difference may be due to the heterogeneous properties of DOS collectors [4].

The depth profiles were deconvoluted by implantation profiles of given kinetic energies, which are calculated by SRIM/TRIM simulation, in order to derive SW velocity distribution. The energies were chosen to model H velocities of 200 to 3500 km s^{-1} with ~100 km s^{-1} intervals. The velocity distribution for the SW H data was determined up to 3000 km s^{-1} (a calculation requiring a dynamic range > 5 orders magnitude (Fig. 3)). A SW H speed of ~400 km s^{-1} dominates the *Genesis* collection period in both B/C and CME chips. This confirms that the algorithm used for Genesis array deployment collected a significant contribution of non-CME SW in the E-array [5]. SW H traveling over 1000 km s^{-1}, correspond to the tails of the depth profiles, show the same distribution for the both collectors. These are H from CME flows which, using ACE/SWICS data [5], have been identified as corresponding to the Halloween solar storms of 2003.

The velocity distribution of SW ^{4}He has been determined over ranges to 1600 km s^{-1} [2]. He/H ratios were determined as a function of SW velocity and normalized to the He/He at 440 km s^{-1} (Fig. 4). The He/H ratios are 2–3 times higher in the CME flow than in the low- and high-speed flow. The enhancement of He/H ratio in the CME flow would be caused by characteristic particle acceleration mechanisms of CME or by propagation mechanisms of interplanetary CME.

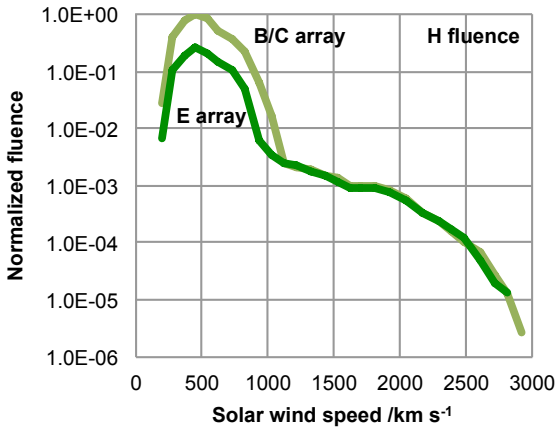

Figure 3. Velocity distribution of solar wind hydrogen determined from Genesis B/C and E DOS collectors.

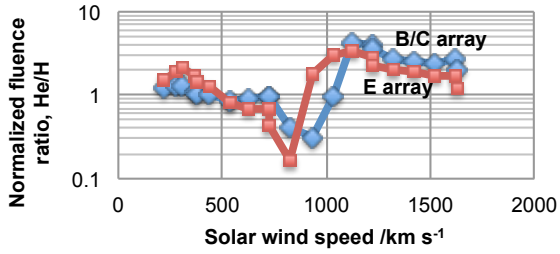

Figure 4. He/H abundance ratio (normalized to low-speed flow) of solar wind as a function of the velocity.

References: [2] Bajo K. et al. (2015) *Geochem. J. 49,* 559–566. [2] Yurimoto H. et al. (2017) *Meteoritics & Planet. Sci., 52,* S1, Abstract #6228. [3] Koeman-Shields E. C. et al. (2016) *LPS XLVII,* Abstract #2800. [4] Koeman-Shields E. C. et al. (2017) *Meteoritics & Planet. Sci., 52,* S1, Abstract #6142. [5] Reisenfeld, D. B., et al. (2013) *Space Sci. Rev. 175,* 125-164.